chosen one point crossover operator, and a mutation operator with elitist strategy as in the simple genetic algorithm given in [4]. The goal of the elitist strategy is to carry the best string from the previous iteration into the next. Therefore, in each iteration, the bits with value 1 in the remaining chromosome are preserved if they satisfy the consistency criteria (i.e. $|w_a^i - w_a^j| < \frac{1}{m^2}\sum_{a=1}^{m}\sum_{b=1}^{m}|w_a^i - w_b^j|$, $i, j = 1 \ldots N_s$, $i \neq j$). Otherwise, they are cleared to 0. Since the positions of the extrema detected in the finer scales are more accurate than those detected in the coarser scales, the bit in the last chromosome which corresponds to the maximum local extremum in the finest scale is chosen as the exact boundary point. After obtaining the exact extremum location on each search line, the B-spine technique is consequently used to construct the desired contour of specific features.

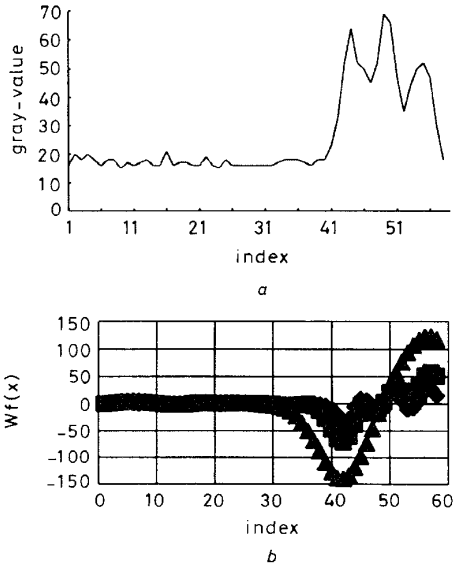

Fig. 1 *Example profile and its three-scales WT*

a Example profile
b Three-scales WT
◆ scale 1
■ scale 2
▲ scale 4

Results: For each image, an arbitrary point inside an ROI is selected and a radial search method is therefore used to extract the contour of the tissue interface at every 5° (this value depends on the complexity of the target contour). The parameters used for GAs are $N_s = 3$, $m = 5$, $N_p = 10$, and mutation rate = 0.01. One of the profiles radiated from a selected point and three-scales WT of this profile are shown in Fig. 1*a* and *b*, respectively. Fig. 2*a* shows an image where the contour of the tumour has been detected by conventional radial search with edge detector. The result using the proposed GAs-based algorithm is illustrated in Fig. 2*b*. It is clear that the contours of the tumour follow the desired object boundary very well when the proposed method is used. Although three-scale WT is sufficient for our applications, the proposed method can be applied to other applications which required large-scale WTs. Furthermore, this algorithm has been implemented in our ultrasonic imaging analysis system (UIAS), which is currently used as an assistant diagnostic tool for tumour detection in the Chang Gung Hospital. The computation time necessary to determine the boundary and the area of the tumour in an ultrasonic image with this method is ~8s on a 80586-90 MHz PC.

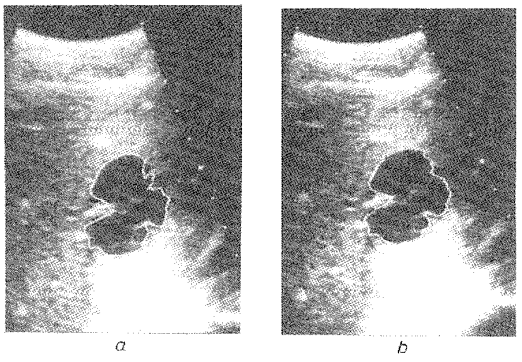

Fig. 2 *Contour extraction performance*

a Image where contour of tumour has been detected by conventional radial search with edge detector
b Result using proposed GAs-based algorithm

Conclusions: In this work, a multi-resolution approach based on WT is introduced to demonstrate contour extraction from an ultrasonic image. The performance of this method has been shown to resolve the ambiguities encountered with the conventional snake algorithms efficiently. More important, the best wavelet features for profile analysis can be estimated by GAs without manual operation. This merit makes the proposed methods more flexible and easy to use than the previous approaches which require complex image preprocessing.

Acknowledgment: This research is supported in part by the National Science Council, ROC under Grant NSC85-2331-B182-087-M08.

16 September 1996
Electronics Letters Online No: 19961434

Jiann-Der Lee (*Department of Electrical Engineering, Chang Gung College of Medicine and Technology, Tao-Yuan, Taiwan 333, Republic of China*)

References

1 KASS, M., WITKIN, A., and TERZOPOULOS, D.: 'Snakes: active contour models', *Int. J. Comput. Vision*, 1988, **1**, pp. 321–331
2 GOLDBERG, D.: 'Genetic algorithms in search, optimization and machine learning' (Addison-Wesley, MA, 1989)
3 MALLAT, S., and ZHONG, S.: 'Characterization of signals from multiscale edges', *IEEE Trans. PAMI*, 1992, **14**, pp. 710–732
4 RUIZ, E.E.S., and FAIRHURST, M.C.: 'Improved approach to boundary location in 2D echocardiographic images', *IEE Proc. Vis. Image Sig. Process.*, 1995, **142**, (3), pp. 121–127

Quantitative images of large biological bodies in microwave tomography by using numerical and real data

J.J. Mallorquí, N. Joachimowicz, A. Broquetas and J.Ch. Bolomey

Indexing terms: Microwave imaging, Computerised tomography

A new inverse microwave imaging algorithm is presented which has the ability to obtain quantitative dielectric maps of large biological bodies. By using *a priori* information, obtained with a first order algorithm, the final image is obtained by solving the direct problem and an ill-conditioned system of equations into an iterative procedure. The algorithm has been successfully tested with real data from an experimental scanner.

Introduction: A microwave imaging system illuminates a body with a well known incident field and measures the diffracted (total) field caused by the body in its proximity. The scattered field obtained by subtracting the incident from the diffracted field can be related to the body permittivity by using a bidimensional TM representation of fields and currents by neglecting depolarisation effects in the explored body. Several geometries of measurement have been proposed for biomedical imaging systems: linear, planar and circular. The latest geometry was adopted in a scanner prototype using a circular array of probes working in the 2.45GHz band built at the Universitat Politècnica de Catalunya [1]. The system has been used to assess several clinical applications using first

order weak scattering algorithms [2 – 5], however, tests pointed out that future progress in this area would be strongly conditioned to the development of new algorithms which are able to reconstruct the high contrast map of tissue permittivities from realistic noisy data.

Imaging algorithms: The reconstruction of the permittivity image from the measured fields belongs to the set of so-called inverse problems, which have some intrinsic difficulties. First, we can only measure the scattered fields produced for each direction of incidence in a limited zone of the space, basically the antenna array, the antenna domain, but not inside the explored body, the object domain. Secondly, the propagation of electromagnetic waves in objects with dimensions of a few wavelengths cannot be modelled as ray propagation and diffraction effects have to be considered. Finally, mainly in the biological case, the problem is 'ill-conditioned': owing to the high contrast of biological tissues and its attenuation, the contribution of the inner body regions to the scattered fields will be easily masked by the huge scattering of the external layers. All those effects contribute to the difficulty of developing efficient inverse algorithms.

The first approaches were based on the Born approximation that assumes a weak scattering situation; the total field inside the body is approximated by the incident field, allowing the inversion problem to be formulated as a mapping of field data on the bi-dimensional Fourier spectrum the image [6]. The images obtained with this algorithm are, in the best case, only qualitative. In biomedical applications, this algorithm often allows us to obtain the shape of the object but not the inner distribution of tissues.

A new algorithm has been proposed [7] consisting of the linearisation of the inverse problem by using a spatial iterative algorithm based on Newton-Kantorovich's procedure. The iterative procedure that allows us to obtain the contrast map of an unknown body from its scattered fields can be summarised as follows:

(i) The algorithm starts with an initial distribution of contrast by using *a priori* information. In this Letter, the shape of the body obtained from the first order Born algorithm and a homogeneous permittivity value has been used. This *a priori* information is necessary to ensure the stability of the iterative process.

(ii) The direct problem, i.e. the computation of the total field over the object and the scattered fields on the receiving antennas, is solved for each direction of incidence, or view, by using the present contrast distribution. The dielectric contrast $C(\vec{r})$ is the relative difference between the complex permittivity of each point of the body $\varepsilon(\vec{r})$ and the reference permittivity ε_0 corresponding to the embedding medium: $C(\vec{r}) = 1 - \varepsilon(\vec{r})/\varepsilon_0$.

(iii) The error in scattered fields, i.e. the difference between the measured and computed fields from the contrast distribution, is obtained.

(iv) By applying a Newton type procedure, an ill-conditioned system relating the update contrast to error on the scattered fields is obtained. A least square solution and a standard Tikhonoy regularisation procedure is used to avoid numerical problems [7].

(v) The process is restarted at (ii) until the error in the scattered fields has an acceptable level.

Results: The number of emitting (views) and receiving antennas necessary to obtain good reconstructed images is not evident. Analysis of real and simulated data have shown that a set of data containing all the scattered information of the object can be obtained by sampling the scattered fields fulfilling the Nyquist sampling theorem over a circle containing the explored object (this is a minimum of two samples by wavelength over it), and by using as many views as the number of array antennas. It would seem that it is necessary to have the same, or larger amount of measurements than contrast unknowns for correct behaviour of the inverse algorithm. By using the previous sampling criteria, the algorithm has enough information to correctly reconstruct the contrast/permittivity map, despite the equation system that needs to be solved in (iii) which could become underdetermined if a fine mesh (~0.1 wavelength/cell) is chosen for the inverse problem. This is possible because the adjacent cells are correlated in the inverse problem due to the lowpass filtering effect of the electromagnetic diffraction. When the input data have low noise levels and a large dynamic range, this fine mesh produces better images in objects with sharp features than a coarse one (p.e. 0.3 wavelength/cell), but increases the size of the equation system. Oversampling of the scattered fields (and an increase in the number of views) will produce only slightly better images, because insignificant new information is measured. At the same time, in practice, the antennas near the emitter antenna are not suitable for acting as receivers [1]. This reduces the number of input data to the algorithm and has a lowpass filtering effect on the final image.

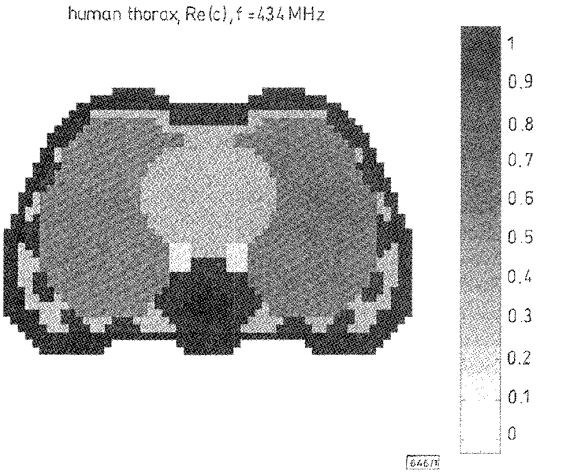

Fig. 1 *Numerical model of human thorax: real part of contrast at 434 MHz*

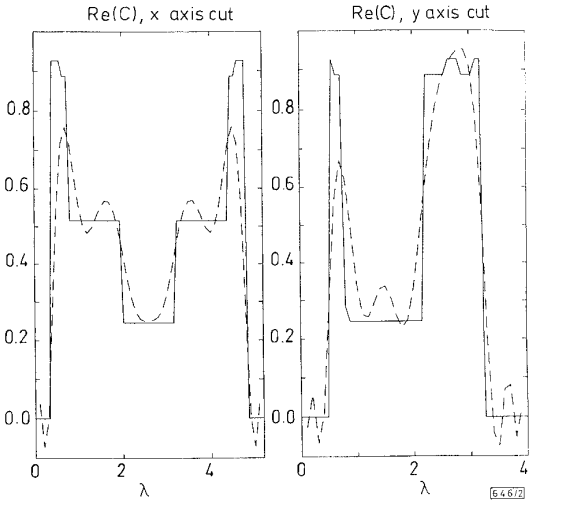

Fig. 2 *Axial cuts of thorax model and reconstructed after nine iterations of real part of contrast*

——— axial
– – – – reconstructed

(i) *Numerical simulation:* The reconstruction of a numerical model of a human thorax with a scanner working at 434MHz and with an array of antennas placed at a radius of 32.4cm has been simulated. The external medium is water, $\varepsilon_0 = 74.0 - j1.1$, and the shape of the body and its lung permittivity are used as *a priori* information (obtained with the first order algorithm). The number of views was chosen from the lower limit of the Nyquist theorem criteria: 32 antennas. Only the 25 antennas (3/4 of the array) in front of the emitting antenna can act as receivers. The reconstruction mesh has a size of 51 by 39 cells with a resolution, in both the direct and the inverse problem, of 0.1 wavelength/cell. Fig. 1 shows the numerical model and Fig. 2 shows two axial cuts of the reconstructed real part of the contrast function after nine iterations.

(ii) *Measured data:* Fig. 3 shows the reconstruction of a human arm measured in the scanner prototype with an estimated signal to noise ratio of 20dB. The external medium is water, $\varepsilon_0 = 77.3 - j8.6$. The reconstruction mesh has a size of 57 by 57 cells with a resolution of 0.1 wavelength/cell in both the direct and inverse

problem. The real part of contrast is presented after five iterations. The reconstructed image shows the position of the two bones and the correct value of muscle contrast (~0.35). Conversely, due to the water and tissue attenuation and lack of dynamic range of the available data, the contrast of bones is lower than the real one (~1.0). It must be pointed out that the limitations on the image quality are mainly due to the data quality, not to the algorithm behaviour.

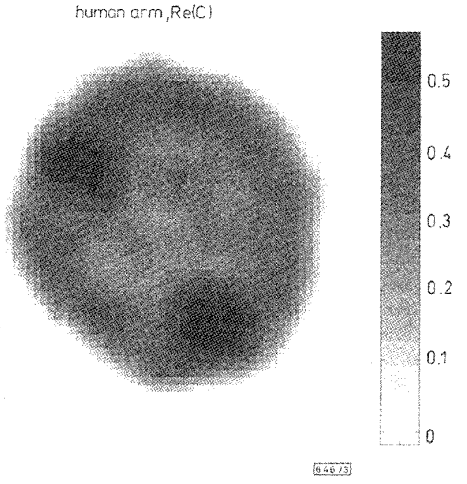

Fig. 3 *Reconstructed human arm from real data after five iterations, real part of contrast*

Conclusions: We have demonstrated the capability of the Newton-Kantorovich algorithm to obtain good quantitative permittivity maps of biological bodies by using real noisy data. The algorithm is stable, despite the ill-conditioning of the problem and the presence of noise, and converges if the sampling of the scattered fields and the number of views fulfills the Nyquist sampling theorem. A first order approximation of the shape of the object and an estimation of its average permittivity are used as *a priori* information.

Acknowledgments: This work has been supported by the Spanish-French Integrated Action No. 253 and by the Comisión Interministerial de Ciencia y Tecnología (CICYT) under Grant TIC 96-0879.

20 September 1996
Electronics Letters Online No: 19961409

J.J. Mallorquí and A. Broquetas (*Department of Signal Theory and Communications, Universitat Politècnica de Catalunya, Campus Nord UPC-D3, C/Gran Capità s/n, 08034 Barcelona, Spain*)

N. Joachimowicz and J.Ch. Bolomey (*Groupe d'Electromagnetisme, SUPELEC/LSS, Ecole Superieure d'Electricite, Plateau de Moulon, 91190 Gif-sur-Yvette, France*)

References

1 BROQUETAS, A., ROMEU, J., RIUS, J.M., ELIAS-FUSTÉ, A., CARDAMA, A., and JOFRE, LL.: 'Cylindrical geometry: A further step in active microwave tomography', *IEEE Trans.*, 1991, **MTT-39**, (5), pp. 836–844

2 BOLOMEY, J.C., and HAWLEY, M.S.: 'Noninvasive control of hyperthermia' *in* GAUTHERIE, M. (Ed.): 'Methods of hyperthermia control' (Springer-Verlag, 1990), Chap. 2, pp. 35–111

3 HAWLEY, M.S., BROQUETAS, A., JOFRE, LL., BOLOMEY, J.CH., and GABORIAUD, G.: 'Microwave imaging of tissue blood content changes', *J. Biomed. Eng.*, 1991, **13**, pp. 197–202

4 JOFRE, LL., HAWLEY, M.S., BROQUETAS, A., DE LOS REYES, E., FERRANDO, M., and ELIAS-FUSTE, A.: 'Medical imaging with a microwave tomographic scanner', *IEEE Trans.*, 1990, **BME-37**, (3), pp. 303–312

5 MALLORQUÍ, J.J., and BROQUETAS, A.: 'Non-invasive active thermometry with a microwave tomographic scanner in hyperthermia treatments', *ACES J., Special Issue on Bioelectromagnetic Comp.*, 1992, **7**, (2), pp. 121–127

6 RIUS, J.M., FERRANDO, M., JOFRE, L., DE LOS REYES, E., ELIAS, A., and BROQUETAS, A.: 'Microwave tomography: An algorithm for cylindrical geometries', *Electron. Lett.*, 1987, **23**, (11), pp. 564–565

7 JOACHIMOWICZ, N., PICHOT, C., and HUGONIN, J.P.: 'Inverse scattering: An iterative method for electromagnetic imaging', *IEEE Trans.*, 1991, **AP-39**, (12), pp. 1742–1752

Speeding up fractal image encoding by wavelet-based block classification

Y. Zhang and L.M. Po

Indexing terms: Fractals, Image coding, Wavelet transforms

The authors propose a novel fast fractal image encoding algorithm using wavelet-based block classfication. The range blocks and corresponding domain blocks are classified into edge selective categories by the energy compacted wavelet coefficients. The searching is carried out between the same classes for range-domain comparisons which significantly reduces the computational complexity. Experimental results show that the proposed method can speed up the fractal image encoding process by up to 12.3 times over the conventional full search method.

Introduction: Since Jacquin introduced the first practical block-based fractal image coding scheme [1] in 1990, fractal coding had aroused a great deal of interest as a new promising image compression technique. However, the encoding complexity of the fractal image coding is extremely high and has became the major limitation for its practical applications. It is well known that the most computationally intensive part of the fractal encoding process is the searching step. This is required for each range block to find the best matched domain block within the searching pool. If the full search (exhaustive search) method is used, the fractal encoding complexity is always dominated by this searching process. As a result, many fast searching algorithms have been developed to alleviate the heavy computation of full-search. Block classification [1, 2] is the most commonly used method in speeding up the searching process. The main idea of block classification is to categorise the range and domain blocks into different classes according to the image features such as mean, variance, moment and other perceptual or statistical geometric features. The searching process is then restricted to the same cluster, that is, only those domain blocks which belong to the same category as the encoded range block will be matched and others are not considered. The computational complexity is reduced because fewer domain blocks are compared with a given range block. The effectiveness of block classification depends on whether the classified features are invariant after affine transformation. In this Letter, a new wavelet-based block classification scheme is proposed to speed up conventional full-search fractal image encoding.

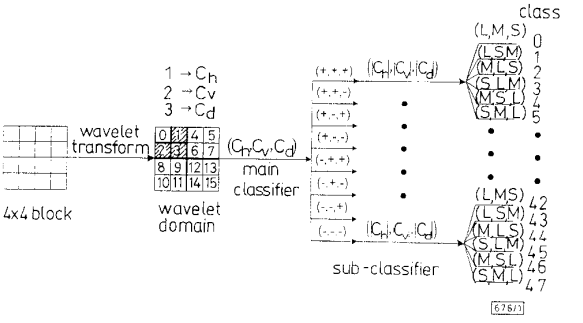

Fig. 1 *Simplified block diagram of wavelet based classification for 4 × 4 image blocks*

Signs '+' and '–' denote positive and negative value of C_h, C_v and C_d, respectively
L, M and S mean largest, middle and smallest absolute magnitude among three values of $|C_h|$, $|C_v|$ and $|C_d|$, respectively

Wavelet-based block classification (WBC): In the discrete wavelet transform (DWT) [3] of 2D image signals, a pair of lowpass and highpass filters is applied separately along the horizontal and